Journal of Neuroimmunology 281 (2015) 44–50

Contents lists available at ScienceDirect

Journal of Neuroimmunology

journal homepage: www.elsevier.com/locate/jneuroim

Associations between changes in ferritin levels and susceptibility-weighted imaging filtered phase in patients with relapsing–remitting multiple sclerosis over 24 weeks of therapy with subcutaneous interferon beta-1a three times weekly

Michael G. Dwyer [a,b,*], Robert Zivadinov [a,b], Silva Markovic-Plese [c,d], Niels Bergsland [a], Mari Heininen-Brown [a], Ellen Carl [a], Cheryl Kennedy [a], Bianca Weinstock-Guttman [e], Brooke Hayward [f], Fernando Dangond [f]

[a] Buffalo Neuroimaging Analysis Center, Department of Neurology, School of Medicine and Biomedical Sciences, University at Buffalo, State University of New York at Buffalo, 100 High St., Buffalo, NY 14203, USA
[b] MR Imaging Clinical Translational Research Center, School of Medicine and Biomedical Sciences, University at Buffalo, State University of New York, 100 High St., Buffalo, NY 14203, USA
[c] Department of Neurology, University of North Carolina at Chapel Hill, 125 Mason Farm Rd., 6109D Neuroscience Research Bldg, CB #7125, Chapel Hill, NC 27599, USA
[d] Department of Microbiology and Immunology, University of North Carolina at Chapel Hill, 125 Mason Farm Rd., 6109D Neuroscience Research Bldg, CB #7125, Chapel Hill, NC 27599, USA
[e] Baird MS Center, Department of Neurology, State University of New York at Buffalo, 100 High St., Buffalo, NY 14203, USA
[f] EMD Serono, Inc., One Technology Pl., Rockland, MA 02370, USA

ARTICLE INFO

Article history:
Received 23 December 2014
Received in revised form 24 February 2015
Accepted 2 March 2015

Keywords:
Multiple sclerosis
Iron deposition
MRI

ABSTRACT

Subanalysis of a pilot study (NCT01085318) assessed correlations between serum ferritin and imaging assessments in relapsing–remitting multiple sclerosis patients (n = 23) receiving 44 μg interferon beta-1a subcutaneously three times weekly. At baseline, 12, and 24 weeks, mean ferritin was 75, 127 ($p < 0.001$ vs baseline), and 101 ($p = 0.020$ vs baseline) ng/mL. No relationship between ferritin and susceptibility-weighted imaging (SWI)-filtered phase of subcortical deep gray matter was found. Increasing ferritin correlated with decreasing lesion numbers on both fluid attenuated inversion recovery and SWI phase at 12 weeks ($r = -0.62$; $p = 0.003$; $n = 21$), and with decreasing gadolinium-enhancing lesion volume at 24 weeks ($r = -0.71$; $p = 0.050$; $n = 8$).

1. Introduction

Ferritin is the principal intracellular iron storage protein, acting as a buffer both to ensure that iron is available when needed and to prevent iron overload. Each of these roles is vital: iron is essential for a number of key metabolic processes, including oxidative phosphorylation and DNA synthesis; it is also integral to the formation of myelin (Da Costa et al., 2011). However, excessive iron produces damaging reactive oxygen species through the Fenton reaction. Increased serum ferritin is usually associated with inflammation, infections, and malignancies, where it is thought to play an adaptive role by reducing the availability of iron to malignant cells. However, increases have also been correlated with disease activity in autoimmune diseases such as systemic lupus erythematosus (Zandman-Goddard and Shoenfeld, 2008).

Hyperferritinemia has also been reported in patients with multiple sclerosis (MS); in particular, serum ferritin levels have been found to be abnormally increased in patients with progressive MS (Da Costa et al., 2011; Sena et al., 2008). However, previous investigations have found patients with stable or relapsing–remitting MS (RRMS) to show no significant ferritin elevation versus healthy controls (Da Costa et al., 2011; Sena et al., 2008). Up-regulation of ferritin expression may be a protective response against oxidative damage from free iron (LeVine and Chakrabarty, 2004; Sena et al., 2008), and apoferritin has been shown to reduce disease activity in an animal model (LeVine et al., 2002). Previous research has shown that interferon beta-1a administered subcutaneously three times weekly (IFN β-1a SC tiw) increases serum ferritin level in patients with RRMS in follow-up up to 12 months after beginning treatment, although no correlation with clinical outcomes was seen in the 43 patients studied and magnetic resonance imaging (MRI) imaging was not performed (Sena et al., 2008).

Susceptibility-weighted imaging (SWI)-filtered phase, an indirect measure indicative of iron deposition, is particularly useful for obtaining images within subcortical deep gray matter (SDGM) tissue (Haacke

* Corresponding author at: Buffalo Neuroimaging Analysis Center, Department of Neurology, School of Medicine and Biomedical Sciences, State University of New York at Buffalo, 100 High St., Buffalo, NY 14203, USA.
E-mail addresses: mgdwyer@bnac.net (M.G. Dwyer), rzivadinov@bnac.net (R. Zivadinov), markovics@neurology.unc.edu (S. Markovic-Plese), npbergsland@bnac.net (N. Bergsland), mari.hhb@live.com (M. Heininen-Brown), ecarl@bnac.net (E. Carl), ckennedy@bnac.net (C. Kennedy), Bweinstock-guttman@kaleidahealth.org (B. Weinstock-Guttman), brooke.hayward@emdserono.com (B. Hayward), fernando.dangond@emdserono.com (F. Dangond).

http://dx.doi.org/10.1016/j.jneuroim.2015.03.002
0165-5728/

et al., 2009a; Hagemeier et al., 2013b). An SWI approach provides more sensitive detection of tissue changes indicative of iron than may be obtained with T2 hypointensity or relaxometry measurements (Haacke et al., 2004, 2009b; Zivadinov et al., 2012). Changes in SWI-filtered phase can be used to provide additional information to complement more traditional MRI measurements, such as T1 and gadolinium-enhancing (Gd+) lesions.

Perhaps due to the recency of phase imaging, the complex relationship between the immune system, ferritin, and brain iron in vivo is poorly understood. To our knowledge, no studies have directly investigated the relationship between changes in ferritin and changes in brain iron. Since ferritin is potentially protective but also upregulated in pathology, it is not even clear a priori whether such relationships (if any) would be positive or negative. Therefore, this substudy was conducted to assess the possible relationship of abnormal (elevated) ferritin levels to SWI and conventional MRI endpoints in patients with RRMS receiving IFN β-1a SC tiw, with the null hypothesis of no relationship between serum ferritin levels and brain iron or MRI endpoints.

2. Material and methods

Data were obtained from a 24-week, non-randomized, open-label, two-arm pilot study (ClinicalTrials.gov ID: NCT01085318) of patients with RRMS receiving IFN β-1a SC tiw (n = 23) and healthy controls (n = 15) (Zivadinov et al., 2014). The trial was conducted in accordance with the International Conference on Harmonization guidelines for Good Clinical Practice and applicable local regulations, as well as the Declaration of Helsinki. Patients gave written informed consent before participation and the protocol was approved by the University at Buffalo Health Sciences Institutional Review Board. Screening occurred within 2 weeks before a patient entered the study.

Patients were eligible for inclusion if they were 18–65 years old, with a diagnosis of RRMS according to the McDonald 2010 criteria (Polman et al., 2011) and disease duration <20 years, and were treatment-naïve or using any of the US Food and Drug Administration-approved disease-modifying drugs (except natalizumab, mitoxantrone, or IFN β-1a SC tiw). Patients were excluded if they had had a relapse within 30 days prior to screening or had received any of the following treatments: IFN β-1a SC tiw, intravenous immunoglobulin, or plasmapheresis within 3 months prior to screening; immunosuppressant agents (eg, mitoxantrone) or any other concomitant immunomodulatory therapies (eg, natalizumab) within 30 days prior to screening; or steroid treatment within 30 days prior to MRI. Other key exclusion criteria were: alanine aminotransferase > 2.5 × upper limit of normal (ULN), alkaline phosphatase > 2.5 × ULN, total bilirubin > 1.5 × ULN, total white blood cell count < 3.0×10^9/L, platelet count < 75×10^9/L, hemoglobin < 100 g/L, complete transverse myelitis, simultaneous-onset bilateral optic neuritis, thyroid dysfunction, moderate-to-severe renal impairment, history of seizures not adequately controlled by treatment, and any serious or acute cardiac disease.

Baseline assessments included physical and neurological exams, MRI scans, and laboratory tests. Blood was drawn for standard laboratory assessments (including iron) and special chemistries (including ferritin) at screening, 12 weeks, and 24 weeks; samples were sent to a central laboratory (Quest Diagnostics, Pittsburgh, PA, USA). Neuroimaging assessments were performed at baseline, Week 12, and at the Week 24/Exit Visit. MRI analyses were rater-blinded. Neurological examinations (which were not blinded) were conducted at screening and the Week 24/Exit Visit. Patients received a safety evaluation telephone call at Week 28 (4 weeks after study exit). Patients received IFN β-1a SC tiw for 24 weeks titrated over 4 weeks to a final dose of 44 μg.

2.1. Data collection

All MRI scans were carried out on a 3 Tesla (3 T) GE Signa Excite HD 12.0 (General Electric, Milwaukee, WI, USA) using a multi-channel head and neck coil. SWI was acquired using a three-dimensional flow-compensated gradient echo sequence with 64 slices, 2-mm slice thickness, field of view (FOV) = 25.6 cm × 19.2 cm, and an in-plane resolution of 0.5 mm × 1 mm (flip angle = 12°; TE/TR = 22/40 ms; acquisition time = 8:46 min:s, bandwidth = 13.89 kHz) (Zivadinov et al., 2012, 2014). Conventional two-dimensional scans (proton density [PD]/T2, fluid attenuated inversion recovery [FLAIR], and T1 SE pre- and post-contrast) were acquired with consistent voxel size (48 slices of 3-mm slice thickness, with FOV = 25.6 cm, matrix = 256 × 256, and phase FOV = 0.75). Patients received a single dose (0.1 mmol/kg) of Gd contrast. Moreover, a three-dimensional high-resolution T1-weighted image (WI) fast spoiled gradient echo sequence with a magnetization-prepared inversion recovery pulse was acquired (TE/TI/TR = 2.8/900/5.9 ms, flip angle = 10°) using 184 1-mm slices, resulting in isotropic resolution. All scans were prescribed parallel to the subcallosal line in an axial-oblique orientation with a single average.

Segmentation of SDGM structures for SWI analysis was done using FMRIB's Integrated Registration and Segmentation Tool (FIRST) on the three-dimensional T1-WI (Patenaude et al., 2011). Additional structures (red nucleus, pulvinar nucleus, and substantia nigra) not identifiable by this method were manually delineated on the most representative SWI-filtered phase slice using JIM5 (Xinapse Systems Ltd., Northamptonshire, UK), as reported previously (Zivadinov et al., 2012). Resulting segmentations were subsequently aligned to SWI phase images using a combination of FSL's linear image registration tool (FLIRT) and non-linear image registration tool (FNIRT). An overview of the analysis method and reproducibility results used in the present study is discussed elsewhere (Zivadinov et al., 2012). Fig. 1 shows SWI-filtered phase of the SDGM, with representative segmented regions overlaid.

Phase white matter (WM) lesions were classified using a manual region-of-interest approach previously shown to be reproducible (Hagemeier et al., 2012, 2014). Image analyses were carried out by a single operator who was blinded to clinical status. WM lesions were identified separately on T2/PD/FLAIR, T1-WI, and SWI-filtered phase maps without a priori knowledge of where the WM lesions were located with respect to the other modalities. Only round/oval WM lesions ≥3 mm in diameter were included in the study. In addition, a

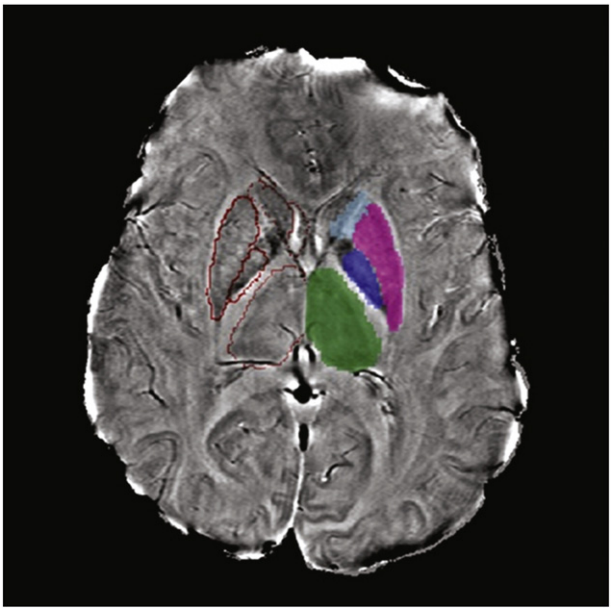

Fig. 1. Representative SWI phase image with specific segmented structures overlaid (thalamus in green, putamen in magenta, globus pallidus in dark blue, and caudate in light blue). On the left side of the figure, outlines are shown to allow visualization of the phase content of structures. Darker regions are indicative of higher susceptibility and potentially higher iron content. SWI: susceptibility-weighted imaging.

subset of WM lesions was visible on both SWI-filtered phase and T2/PD/FLAIR, and a subset was visible on both SWI-filtered phase and T1-WI; these were identified a posteriori as overlapping when one or more voxels overlapped after unblinding was performed.

Images and WM lesion maps for each patient were co-registered with FMRIB's FLIRT using 6-degrees-of-freedom (rigid-body) (Jenkinson and Smith, 2001). Images were re-sampled using tri-linear interpolation and WM lesion maps were re-sampled with nearest-neighbor interpolation using the registration matrix from their source images. A semi-automated edge detection contouring/thresholding technique was used to identify WM lesions (Zivadinov et al., 2001, 2012).

Post-processing of the SDGM was performed to identify voxels likely to contain abnormally high amounts of iron based on their phase values. Reference phase values for each SDGM structure were determined previously using a large sample of healthy controls (Zivadinov et al., 2012). Only the voxels of SDGM structures with phase values lower than two standard deviations (SDs) below the reference group were retained, yielding structure-specific maps of voxels with abnormally low phase. Subsequently, as a measure of the level of phase decrease, the mean value of sub-threshold voxels was calculated to yield the mean phase of low phase voxels (MP-LPV). Mean phase and MP-LPV values were calculated in radians, with lower mean phase and MP-LPV values suggesting increased iron content.

2.2. Statistical methods

Sample size was based on clinical rather than statistical considerations. Twenty-five patients with RRMS were planned for inclusion in the intent-to-treat population (Zivadinov et al., 2014). Changes in serum ferritin and iron levels from baseline to Week 12 and Week 24 for patients with RRMS were analyzed using paired *t*-tests. The possible relationship of change in ferritin levels with iron levels and with MRI endpoints was assessed in patients with RRMS using Spearman's correlation coefficient.

3. Results

Demographic and baseline characteristics of patients with RRMS are shown in Table 1.

3.1. Changes in ferritin and iron levels

Of the 23 enrolled patients, ferritin levels were missing for one patient at 12 weeks and for one other patient at 24 weeks. Mean (SD) ferritin at baseline was 74.7 (75.30) ng/mL; this increased to 127.2 (109.18) ng/mL at 12 weeks ($p < 0.001$ vs baseline) and decreased to 101.2 (99.57) ng/mL at 24 weeks ($p = 0.020$ vs baseline; $p = 0.034$ vs 12 weeks). Fig. 2 shows changes in ferritin levels over the course of the study. Ferritin level at 12 weeks was higher than at baseline for all but one patient (out of 22). Ferritin levels for 15/21 patients decreased from 12 to 24 weeks but were still above baseline levels at Week 24 for 15/22 patients. Ferritin levels were elevated above the ULN range (232 ng/mL for women and 345 ng/mL for men) for only one woman (at Week 12 only) and one man (at Weeks 12 and 24).

At baseline, mean (SD) serum iron level was 87.7 (36.97) μg/dL; over 12 weeks this decreased to 84.0 (40.26) μg/dL ($p = 0.652$). By 24 weeks, serum iron increased to a mean of 96.7 (39.29) μg/dL, a mean increase of 8.1 (39.80) μg/dL from baseline ($p = 0.351$ vs baseline). No correlation was seen between serum iron and ferritin levels at any timepoint ($r = 0.04$ [$p = 0.866$] at baseline; $r = -0.26$ [$p = 0.248$] at Week 12; and $r = 0.17$ [$p = 0.457$] at Week 24).

3.2. Ferritin and MRI endpoints

No relationship between changes in serum ferritin and SWI-filtered phase of the SDGM was found. Fig. 3 shows change in ferritin and MP-LPV of the entire SDGM from baseline to Week 24. No significant change from baseline was seen in MP-LPV of the SDGM (mean [SD] Week 24 change from baseline, 0.0009 [0.0217] radians).

There was an inverse correlation ($r = -0.62$; $p = 0.003$; $n = 21$) between change in ferritin level and the number of overlapping SWI phase and FLAIR lesions after 12 weeks of therapy (i.e., as ferritin level increased, the number of overlapping SWI phase and FLAIR lesions decreased; Fig. 4A). There was no correlation between these two measures after 24 weeks (Fig. 4B).

There was a borderline statistically significant positive correlation ($r = 0.44$; $p = 0.047$; $n = 21$) between ferritin level and absolute change in T1 lesion volume after 24 weeks (ie, increase in ferritin level correlated with an increase in T1 lesion volume; Fig. 5). There was also a borderline significant negative correlation ($r = -0.71$; $p = 0.050$) between ferritin and percentage change in Gd+ lesion volume after 24 weeks among the eight patients with Gd+ lesions at baseline (Fig. 6). No other significant correlations were seen between changes in serum ferritin level and lesion number or volume.

Table 1
Baseline characteristics and drug exposure/compliance of patients with RRMS.

	Patients with RRMS
	n = 23
Mean (SD) age, years	39.9 (10.17)
Female, n (%)	14 (61)
Race, n (%)	
Caucasian	20 (87)
African American	3 (13)
Mean (SD) years since MS diagnosis, range	6.6 (5.65), 0–20
Mean (SD) years since most recent relapse, range	1.0 (1.14), 0.1–5.0
Mean (SD) number of relapses in past 12 months[a]	1.3 (1.18)
0, n (%)	7 (30)
1, n (%)	7 (30)
2, n (%)	7 (30)
4, n (%)	2 (9)
Most recent DMD use, n (%)	
IFN β-1a IM	8 (35)
IFN β-1a SC	5 (22)
Glatiramer acetate	4 (17)
Natalizumab	2 (9)
IV immunoglobulin	1 (4)
None	3 (13)
Median (range) EDSS score	2.5 (1–5.5)
Mean (SD) serum ferritin, ng/mL	74.7 (75.30)

	Mean (SD)	Median (range)
T2 lesion number	34.9 (24.51)	28.0 (5.0–115.0)
T2 lesion volume, mm^3	23,683 (27,730.6)	17,739 (558–118,940)
T1 lesion number	19.5 (15.34)	19.0 (0.0–59.0)
T1 lesion volume, mm^3	4532 (5417.4)	2847 (0–23,364)
Gd + lesion number	1.8 (4.84)	0.0 (0.0–22.0)
Gd + lesion volume, mm^3	240 (646.4)	0 (0–2915)
SWI lesion number	17.4 (14.47)	16.5 (2.0–68.0)
SWI lesion volume, mm^3	2620 (2289.6)	2553 (43–9763)
Number of lesions on overlapping SWI and FLAIR	16.6 (15.03)	16.5 (1.0–71.0)
Volume of lesions on overlapping SWI and FLAIR, mm^3	1342 (1555.9)	984 (11–6811)

Study drug exposure and compliance[b]	IFN β-1a SC tiw n = 23		
	8.8 μg	22 μg	44 μg
Mean (SD) total dose received, μg	52.5 (7.60)	133.9 (9.17)	2174.9 (584.47)
Mean (SD) doses missed	0 (0.2)	0 (0)	5 (7.6)
Mean (SD) compliance, %	99 (3.5)	100 (0)	92 (12.2)

DMD: disease-modifying drug; EDSS: Expanded Disability Status Scale; FLAIR: fluid attenuated inversion recovery; Gd+: gadolinium-enhancing; IFN β-1a: interferon beta-1a; IM: intramuscularly; IV: intravenous; MS: multiple sclerosis; RRMS: relapsing–remitting multiple sclerosis; SC: subcutaneously; SD: standard deviation; SWI: susceptibility-weighted imaging; tiw: three times weekly.

[a] Patients reported the same number of relapses for the past 24 months.

[b] Compliance was calculated at study visits using patient diaries and returned drug.

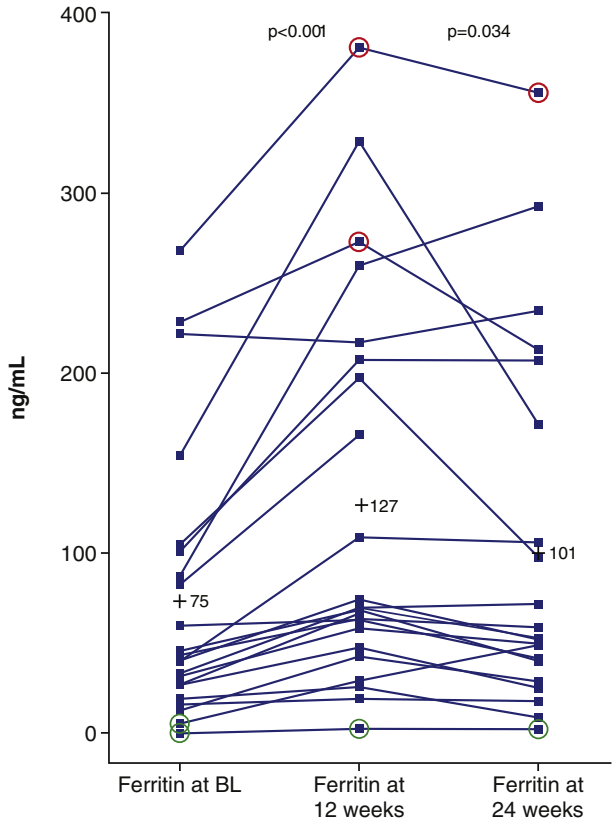

Fig. 2. Ferritin levels over the course of the study. "+" signs represent mean serum ferritin values observed at each timepoint (75, 127, and 101 ng/mL at BL, 12 weeks, and 24 weeks respectively); p-values are for the change from 0 to 12 weeks and 12 to 24 weeks. Red circles represent values above the upper limit of normal (232 ng/mL for women [one patient at Week 12 only] and 345 ng/mL for men [one patient at Weeks 12 and 24]); green circles represent values below the lower limit of normal (10 ng/mL for women [one patient for all timepoints and one patient at BL only]; no measurements were below the lower limit of normal for men in this study). BL: baseline.

3.3. Safety and tolerability

Almost all patients with RRMS (22/23) had ≥1 treatment-emergent adverse event, as previously reported (Zivadinov et al., 2014). As expected, injection-site reactions and influenza-like illness were the most commonly occurring events.

4. Discussion

In this substudy of a 24-week, non-randomized, single-center trial, patients with RRMS experienced increases in serum ferritin level after initiation of treatment with IFN β-1a SC tiw. However, these increases did not appear to be associated with increased iron deposition in the SDGM or lesion formation, as assessed by SWI-filtered phase. Previous research has indicated that the effects of IFN β-1a SC tiw include increases in serum ferritin and decreases in early lesion formation (Bastianello et al., 2011; Li et al., 1999; Sena et al., 2008). This is consistent with the observations from this analysis, in which ferritin increase was correlated with reductions in lesions simultaneously visible on FLAIR and SWI-phase, and with reductions in Gd + lesion volume.

In this substudy, changes in serum ferritin were not accompanied by changes in serum iron. Past research has found a lack of serum iron elevation in patients with MS, even among patients with progressive disease who had elevated serum levels of ferritin (Abo-Krysha and Rashed, 2008; Sfagos et al., 2005). Furthermore, since serum iron is subject to active transport via carrier molecules rather than directly crossing the blood–brain barrier (Moos et al., 2007), the relationship between serum iron or ferritin levels and brain iron is complex. For example, in elderly healthy volunteers, a relationship was shown between serum iron and deep gray matter iron, but there was no corresponding relationship with serum ferritin (House et al., 2010). However, in mice fed a short-term iron-overload diet, serum iron and liver iron were significantly increased, but there was no change in brain iron level (Johnstone and Milward, 2010). In this study, we had a unique opportunity to combine blood assays and MRI analysis to study both serum changes and iron-sensitive MRI phase data. SWI-filtered phase is influenced by local magnetic field changes caused by paramagnetic substances such as ferritin, and thus has been proposed as a method of indirectly measuring increases in iron content in vivo (Haacke et al., 2004; Hagemeier et al., 2013a). In this study, decreases in MP-LPV (mean phase values of only those voxels with phase values more than two SDs from the mean value observed among the reference group) (Hagemeier et al., 2013a; Zivadinov et al., 2012) were used as a measure of iron content increase in brain structures. Iron would be the most likely cause of such changes in mean phase measures, although other factors including the diamagnetic properties of myelin and

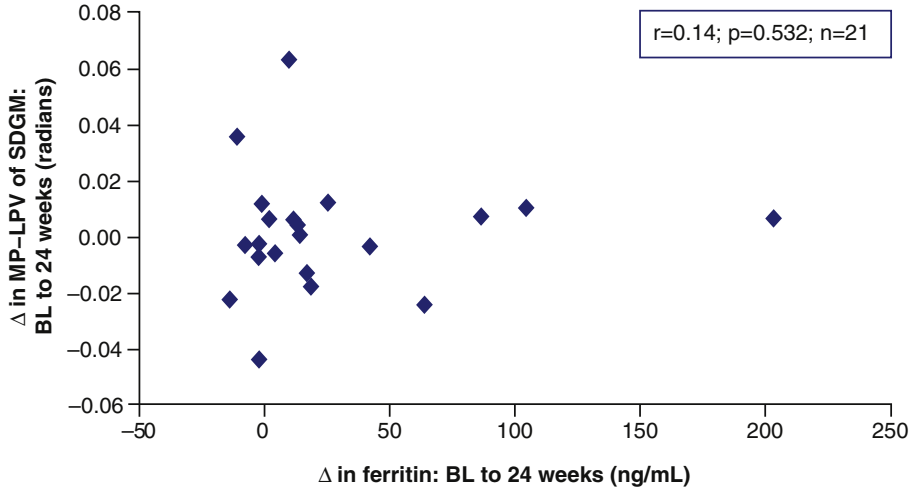

Fig. 3. Change from 0 to 24 weeks in MP-LPV of total SDGM versus change from 0 to 24 weeks in serum ferritin. Lower MP-LPV is indicative of higher iron content. BL: baseline; MP-LPV: mean phase of low phase voxels; SDGM: subcortical deep gray matter.

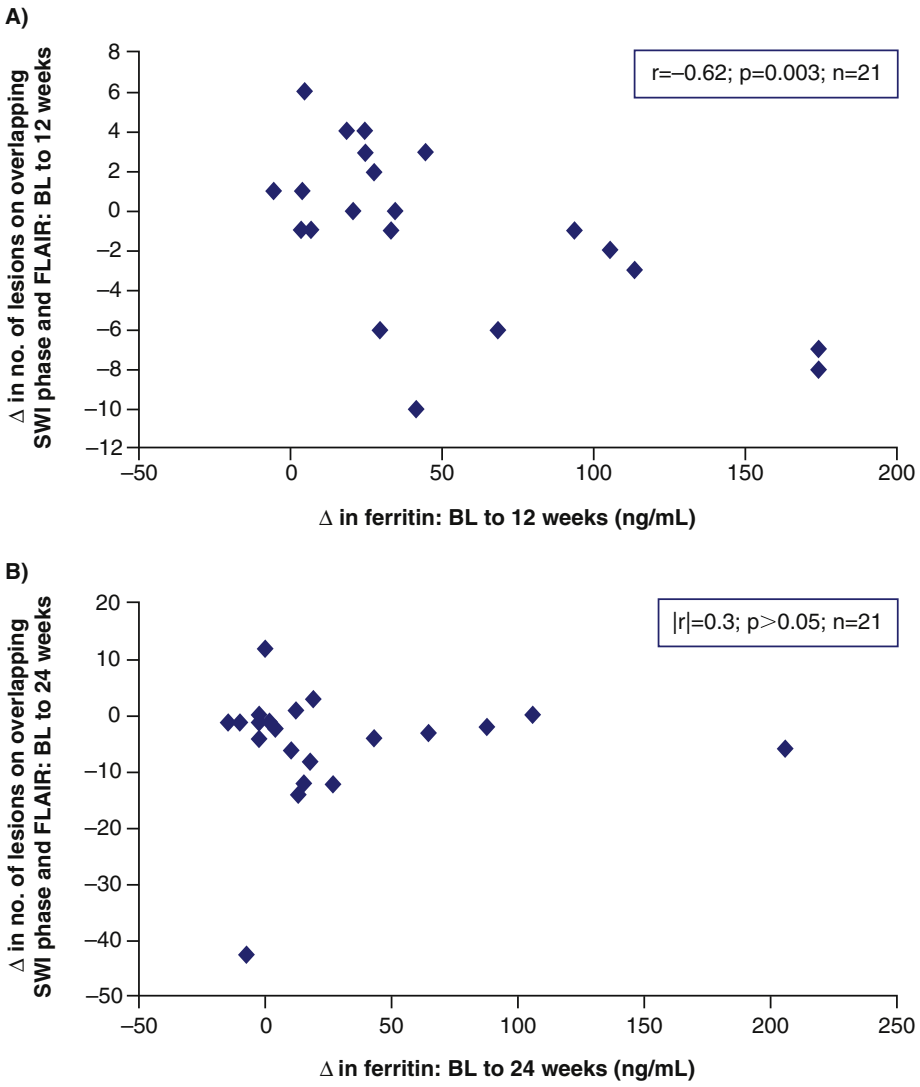

Fig. 4. Change in lesion number on overlapping SWI phase and FLAIR versus change in serum ferritin level over A) 0–12 weeks and B) 0–24 weeks. BL: baseline; FLAIR: fluid attenuated inversion recovery; SWI: susceptibility-weighted imaging.

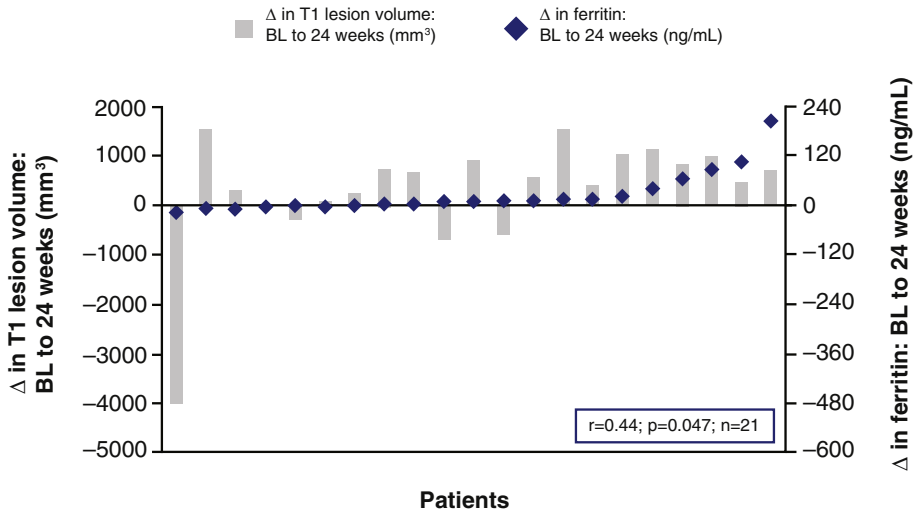

Fig. 5. Change in T1 lesion volume versus change in ferritin over 0–24 weeks. BL: baseline.

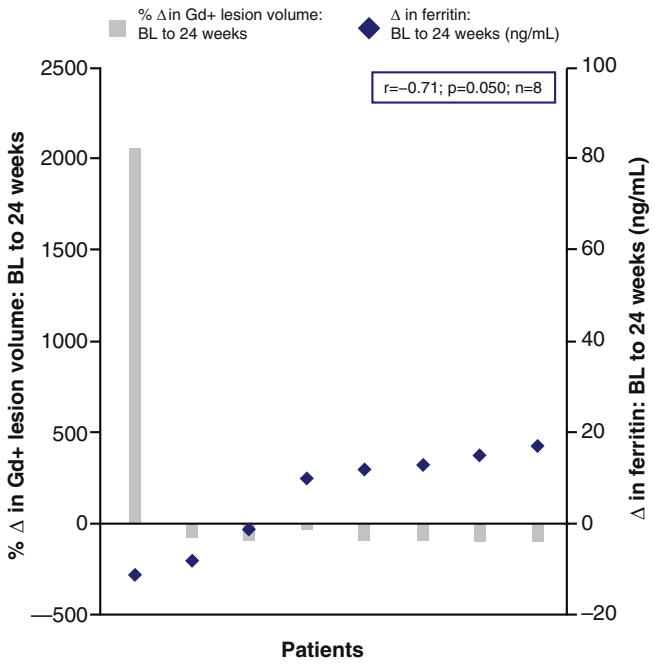

Fig. 6. Percentage change in Gd + lesion volume and change in ferritin over 0–24 weeks. BL: baseline; Gd +: gadolinium-enhancing.

regional atrophy could also potentially influence phase shifts (Bagnato et al., 2011; Langkammer et al., 2010; Yao et al., 2012; Schweser et al., 2011, 2013). After 24 weeks of IFN β-1a SC tiw treatment, the significant changes in ferritin were not accompanied by any significant change in MP-LPV of the SDGM in this study, and there was no correlation observed between changes in MP-LPV in the SDGM and serum ferritin.

There are a number of possible explanations for this lack of correlation. First, the blood–brain barrier may insulate the brain from changes in the serum. Although this has not been directly investigated in MS, cerebrospinal fluid and serum ferritin assessments have yielded dramatically different results in other diseases such as restless leg syndrome (Earley et al., 2000). Second, it is important to note that although MRI phase-based techniques are highly sensitive to iron, they are not able to reliably distinguish among the different forms of iron (e.g., between free iron, transferrin, ferritin, and hemosiderin). Future studies with further advances in MRI techniques may be able to investigate this. Finally, it is important to note that this was a relatively small subanalysis of a pilot study, and subtle changes below our statistical threshold cannot be ruled out.

In MS lesions, oligodendrocyte destruction and demyelination can liberate iron bound to ferritin and permit it to be transformed into reactive species that can amplify oxidative damage and cellular injury (Lassmann, 2011). The precise pathophysiological significance of the iron accumulation seen in some, but not all, MS lesions remains uncertain (Bian et al., 2013; Mehta et al., 2013). It may be indicative of debris from breakdown of myelin or oligodendrocytes, accumulation in microglia/macrophages, or leakage from compromised blood vessels, or it may have a causal role in brain pathology (Haacke et al., 2009a; Mehta et al., 2013; Hametner et al., 2013). Phase lesions may indicate the presence of iron, but they are possibly even more affected by changes in myelin (Bian et al., 2013; Chen et al., 2014; Wen et al., 2014; Yao et al., 2012). The WM lesion changes seen in this study could be related to the dual effect of IFN β-1a SC tiw on both iron and myelin content (Bian et al., 2013; Eissa et al., 2009; Haacke et al., 2009a; Hagemeier et al., 2014; Mehta et al., 2013; Yablonskiy et al., 2012; Yao et al., 2012). It is worthwhile to note that ferritin receptors are abundant in the white matter and that their distribution is reduced in and around MS lesions (Hulet et al., 1999).

From a clinical perspective, the implication of this study is that therapy-related changes in serum ferritin do not appear to have a substantial impact on brain iron homeostasis in the short term. The precise role of iron in multiple sclerosis is still poorly understood, since iron can play a negative role in the formation of reactive oxygen species, but is also essential for oligodendrocyte function and myelination. Therefore, such a lack of interference is potentially comforting in the absence of a precise understanding of ideal brain iron levels.

The short duration and small sample size of this analysis are limitations of this study. No RRMS group receiving placebo was included. However, the results of this study can be used to guide further exploration of effects of therapy on ferritin levels in patients with RRMS and the possible contributions of ferritin and iron to phase lesion development.

5. Conclusions

IFN β-1a SC tiw therapy was associated with short-term increases in serum ferritin levels and reductions in lesions simultaneously visible on FLAIR and SWI phase. This association and the correlation of reduced Gd + lesions with ferritin increase are consistent with previous research that found IFN β-1a SC tiw to increase serum ferritin and decrease early lesion formation, while an explanation for the positive correlation seen between ferritin and T1 lesion volume requires further investigation. The increases in serum ferritin levels seen were not associated with significant increases in serum iron or with concurrent iron deposition in the SDGM, as indicated by SWI. These data suggest that increased serum ferritin after initiation of IFN β-1a SC tiw does not contribute to brain iron accumulation or lesion formation. In fact, the increase in ferritin induced by IFN β-1a SC tiw was associated with a reduction in iron-containing lesions by overlapping SWI and FLAIR, although significant correlation was only seen over the first 12 weeks of treatment.

Conflict of interest statement

MG Dwyer received consulting fees from Claret and EMD Serono, Inc. R Zivadinov received personal compensation from Biogen Idec, Claret, EMD Serono, Inc., Novartis, Sanofi-Genzyme, and Teva Pharmaceuticals for speaking and consultant fees. He also received financial support for research activities from Biogen Idec, Claret, EMD Serono, Inc., Novartis, Sanofi-Genzyme, and Teva Pharmaceuticals. S Markovic-Plese received personal compensation from EMD Serono and Genzyme Inc. for consultant fees. She also received research grants from Biogen Idec, EMD Serono, Genzyme Inc., and Novartis. B Weinstock-Guttman received honoraria as a speaker and a consultant for Acorda, Biogen Idec, EMD Serono, Inc., Genzyme and Sanofi, Novartis, Pfizer, and Teva Pharmaceuticals, and has also received research funds from Acorda, Biogen Idec, EMD Serono, Inc., Genzyme and Sanofi, Novartis, and Teva Pharmaceuticals. B Hayward and F Dangond are employees of EMD Serono, Inc. (a subsidiary of Merck KGaA, Darmstadt, Germany). N Bergsland, M Heininen-Brown, E Carl, and C Kennedy have nothing to disclose.

Role of the funding source

This study was sponsored by EMD Serono, Inc., Rockland, MA, USA (a subsidiary of Merck KGaA, Darmstadt, Germany), and by Pfizer Inc., New York, NY, USA (study number 29665). The principal investigators designed and performed the study, and the sponsor provided central statistical support. All authors revised this report and approved its final version for submission.

Acknowledgments

Rob Coover and Chris Grantham of Caudex Medical, New York, NY, USA, assisted in the preparation of the manuscript and were supported by EMD Serono, Inc., Rockland, MA, USA (a subsidiary of Merck KGaA, Darmstadt, Germany).

References

Abo-Krysha, N., Rashed, L., 2008. The role of iron dysregulation in the pathogenesis of multiple sclerosis: an Egyptian study. Mult. Scler. 14, 602–608.

Bagnato, F., Hametner, S., Yao, B., van Gelderen, P., Merkle, H., Cantor, F.K., Lassmann, H., Duyn, J.H., 2011. Tracking iron in multiple sclerosis: a combined imaging and histopathological study at 7 Tesla. Brain 134, 3602–3615.

Bastianello, S., Giugni, E., Amato, M.P., Tola, M.R., Trojano, M., Galletti, S., Luccichenti, G., Quarantelli, M., Picconi, O., Patti, F., 2011. Changes in magnetic resonance imaging disease measures over 3 years in mildly disabled patients with relapsing–remitting multiple sclerosis receiving interferon beta-1a in the COGnitive Impairment in MUltiple Sclerosis (COGIMUS) study. BMC Neurol. 11, 125.

Bian, W., Harter, K., Hammond-Rosenbluth, K.E., Lupo, J.M., Xu, D., Kelley, D.A., Vigneron, D.B., Nelson, S.J., Pelletier, D., 2013. A serial in vivo 7 T magnetic resonance phase imaging study of white matter lesions in multiple sclerosis. Mult. Scler. 19, 69–75.

Chen, W., Gauthier, S.A., Gupta, A., Comunale, J., Liu, T., Wang, S., Pei, M., Pitt, D., Wang, Y., 2014. Quantitative susceptibility mapping of multiple sclerosis lesions at various ages. Radiology 271, 183–192.

Da Costa, R., Szyper-Kravitz, M., Szekanecz, Z., Csepany, T., Danko, K., Shapira, Y., Zandman-Goddard, G., Orbach, H., Agmon-Levin, N., Shoenfeld, Y., 2011. Ferritin and prolactin levels in multiple sclerosis. Isr. Med. Assoc. J. 13, 91–95.

Earley, C.J., Connor, J.R., Beard, J.L., Malecki, E.A., Epstein, D.K., Allen, R.P., 2000. Abnormalities in CSF concentrations of ferritin and transferrin in restless legs syndrome. Neurology 54, 1698–1700.

Eissa, A., Lebel, R.M., Korzan, J.R., Zavodni, A.E., Warren, K.G., Catz, I., Emery, D.J., Wilman, A.H., 2009. Detecting lesions in multiple sclerosis at 4.7 tesla using phase susceptibility-weighting and T2-weighting. J. Magn. Reson. Imaging 30, 737–742.

Haacke, E.M., Xu, Y., Cheng, Y.C., Reichenbach, J.R., 2004. Susceptibility weighted imaging (SWI). Magn. Reson. Med. 52, 612–618.

Haacke, E.M., Makki, M., Ge, Y., Maheshwari, M., Sehgal, V., Hu, J., Selvan, M., Wu, Z., Latif, Z., Xuan, Y., Khan, O., Garbern, J., Grossman, R.I., 2009a. Characterizing iron deposition in multiple sclerosis lesions using susceptibility weighted imaging. J. Magn. Reson. Imaging 29, 537–544.

Haacke, E.M., Mittal, S., Wu, Z., Neelavalli, J., Cheng, Y.C., 2009b. Susceptibility-weighted imaging: technical aspects and clinical applications, part 1. AJNR Am. J. Neuroradiol. 30, 19–30.

Hagemeier, J., Heininen-Brown, M., Poloni, G.U., Bergsland, N., Magnano, C.R., Durfee, J., Kennedy, C., Carl, E., Weinstock-Guttman, B., Dwyer, M.G., Zivadinov, R., 2012. Iron deposition in multiple sclerosis lesions measured by susceptibility-weighted imaging filtered phase: a case control study. J. Magn. Reson. Imaging 36, 73–83.

Hagemeier, J., Dwyer, M.G., Bergsland, N., Schweser, F., Magnano, C.R., Heininen-Brown, M., Ramasamy, D.P., Carl, E., Kennedy, C., Melia, R., Polak, P., Deistung, A., Geurts, J.J., Reichenbach, J.R., Zivadinov, R., 2013a. Effect of age on MRI phase behavior in the subcortical deep gray matter of healthy individuals. AJNR Am. J. Neuroradiol. 34, 2144–2151.

Hagemeier, J., Weinstock-Guttman, B., Heininen-Brown, M., Poloni, G.U., Bergsland, N., Schirda, C., Magnano, C.R., Kennedy, C., Carl, E., Dwyer, M.G., Minagar, A., Zivadinov, R., 2013b. Gray matter SWI-filtered phase and atrophy are linked to disability in MS. Front. Biosci. (Elite Ed.) 5, 525–532.

Hagemeier, J., Heininen-Brown, M., Gabelic, T., Guttuso, T., Silvestri, N., Lichter, D., Fugoso, L.E., Bergsland, N., Carl, E., Geurts, J.J.G., Weinstock-Gutman, B., Zivadinov, R., 2014. Phase white matter signal abnormalities in patients with clinically isolated syndrome and other neurological disorders. AJNR Am. J. Neuroradiol. 35, 1916–1923.

Hametner, S., Wimmer, I., Haider, L., Pfeifenbring, S., Bruck, W., Lassmann, H., 2013. Iron and neurodegeneration in the multiple sclerosis brain. Ann. Neurol. 74, 848–861.

House, M.J., St Pierre, T.G., Milward, E.A., Bruce, D.G., Olynyk, J.K., 2010. Relationship between brain R(2) and liver and serum iron concentrations in elderly men. Magn. Reson. Med. 63, 275–281.

Hulet, S.W., Powers, S., Connor, J.R., 1999. Distribution of transferrin and ferritin binding in normal and multiple sclerotic human brains. J. Neurol. Sci. 165, 48–55.

Jenkinson, M., Smith, S., 2001. A global optimisation method for robust affine registration of brain images. Med. Image Anal. 5, 143–156.

Johnstone, D., Milward, E.A., 2010. Genome-wide microarray analysis of brain gene expression in mice on a short-term high iron diet. Neurochem. Int. 56, 856–863.

Langkammer, C., Krebs, N., Goessler, W., Scheurer, E., Ebner, F., Yen, K., Fazekas, F., Ropele, S., 2010. Quantitative MR imaging of brain iron: a postmortem validation study. Radiology 257, 455–462.

Lassmann, H., 2011. Mechanisms of neurodegeneration shared between multiple sclerosis and Alzheimer's disease. J. Neural Transm. 118, 747–752.

LeVine, S.M., Chakrabarty, A., 2004. The role of iron in the pathogenesis of experimental allergic encephalomyelitis and multiple sclerosis. Ann. N. Y. Acad. Sci. 1012, 252–266.

LeVine, S.M., Maiti, S., Emerson, M.R., Pedchenko, T.V., 2002. Apoferritin attenuates experimental allergic encephalomyelitis in SJL mice. Dev. Neurosci. 24, 177–183.

Li, D.K., Paty, D.W., UBC MS/MRI Analysis Research Group, PRISMS Study Group, 1999. Magnetic resonance imaging results of the PRISMS trial: a randomized, double-blind, placebo-controlled study of interferon-beta1a in relapsing–remitting multiple sclerosis. Ann. Neurol. 46, 197–206.

Mehta, V., Pei, W., Yang, G., Li, S., Swamy, E., Boster, A., Schmalbrock, P., Pitt, D., 2013. Iron is a sensitive biomarker for inflammation in multiple sclerosis lesions. PLoS One 8, e57573.

Moos, T., Rosengren, N.T., Skjorringe, T., Morgan, E.H., 2007. Iron trafficking inside the brain. J. Neurochem. 103, 1730–1740.

Patenaude, B., Smith, S.M., Kennedy, D.N., Jenkinson, M., 2011. A Bayesian model of shape and appearance for subcortical brain segmentation. Neuroimage 56, 907–922.

Polman, C.H., Reingold, S.C., Banwell, B., Clanet, M., Cohen, J.A., Filippi, M., Fujihara, K., Havrdova, E., Hutchinson, M., Kappos, L., Lublin, F.D., Montalban, X., O'Connor, P., Sandberg-Wollheim, M., Thompson, A.J., Waubant, E., Weinshenker, B., Wolinsky, J.S., 2011. Diagnostic criteria for multiple sclerosis: 2010 revisions to the McDonald criteria. Ann. Neurol. 69, 292–302.

Schweser, F., Deistung, A., Lehr, B.W., Reichenbach, J.R., 2011. Quantitative imaging of intrinsic magnetic tissue properties using MRI signal phase: an approach to in vivo brain iron metabolism? Neuroimage 54, 2789–2807.

Schweser, F., Dwyer, M.G., Deistung, A., Reichenbach, J.R., Zivadinov, R., 2013. Impact of tissue atrophy on high-pass filtered MRI signal phase-based assessment in large-scale group-comparison studies: a simulation study. Front. Phys. 1, 14.

Sena, A., Pedrosa, R., Ferret-Sena, V., Cascais, M.J., Roque, R., Araujo, C., Couderc, R., 2008. Interferon beta therapy increases serum ferritin levels in patients with relapsing–remitting multiple sclerosis. Mult. Scler. 14, 857–859.

Sfagos, C., Makis, A.C., Chaidos, A., Hatzimichael, E.C., Dalamaga, A., Kosma, K., Bourantas, K.L., 2005. Serum ferritin, transferrin and soluble transferrin receptor levels in multiple sclerosis patients. Mult. Scler. 11, 272–275.

Wen, J., Cross, A.H., Yablonskiy, D.A., 2014. On the role of physiological fluctuations in quantitative gradient echo MRI: implications for GEPCI, QSM, and SWI. Magn. Reson. Med. http://dx.doi.org/10.1002/mrm.25114 (Epub ahead of print).

Yablonskiy, D.A., Luo, J., Sukstanskii, A.L., Iyer, A., Cross, A.H., 2012. Biophysical mechanisms of MRI signal frequency contrast in multiple sclerosis. Proc. Natl. Acad. Sci. U. S. A. 109, 14212–14217.

Yao, B., Bagnato, F., Matsuura, E., Merkle, H., van Gelderen, P., Cantor, F.K., Duyn, J.H., 2012. Chronic multiple sclerosis lesions: characterization with high-field-strength MR imaging. Radiology 262, 206–215.

Zandman-Goddard, G., Shoenfeld, Y., 2008. Hyperferritinemia in autoimmunity. Isr. Med. Assoc. J. 10, 83–84.

Zivadinov, R., Rudick, R.A., De Masi, R., Nasuelli, D., Ukmar, M., Pozzi-Mucelli, R.S., Grop, A., Cazzato, G., Zorzon, M., 2001. Effects of IV methylprednisolone on brain atrophy in relapsing–remitting MS. Neurology 57, 1239–1247.

Zivadinov, R., Heininen-Brown, M., Schirda, C.V., Poloni, G.U., Bergsland, N., Magnano, C.R., Durfee, J., Kennedy, C., Carl, E., Hagemeier, J., Benedict, R.H., Weinstock-Guttman, B., Dwyer, M.G., 2012. Abnormal subcortical deep-gray matter susceptibility-weighted imaging filtered phase measurements in patients with multiple sclerosis: a case–control study. Neuroimage 59, 331–339.

Zivadinov, R., Dwyer, M.G., Markovic-Plese, S., Kennedy, C., Bergsland, N., Ramasamy, D.P., Durfee, J., Hojnacki, D., Hayward, B., Dangond, F., Weinstock-Guttman, B., 2014. Effect of treatment with interferon beta-1a on changes in voxel-wise magnetization transfer ratio in normal appearing brain tissue and lesions of patients with relapsing–remitting multiple sclerosis: a 24-week, controlled pilot study. PLoS One 9, e91098.